arXiv:1410.7484v2 [cs.CV] 21 Jan 2015

Abrupt Motion Tracking via Nearest Neighbor Field Driven Stochastic Sampling

Tianfei Zhou[a], Yao Lu[a,*], Feng Lv[a], Huijun Di[a], Qingjie Zhao[a], Jian Zhang[b]

[a] *Beijing Laboratory of Intelligent Information Technology, School of Computer Science, Beijing Institute of Technology, Beijing, China*
[b] *Advanced Analytics Institute, University of Technology, Sydney, Australia*

Abstract

Stochastic sampling based trackers have shown good performance for abrupt motion tracking so that they have gained popularity in recent years. However, conventional methods tend to use a two-stage sampling paradigm, in which the search space needs to be uniformly explored with an inefficient preliminary sampling phase. In this paper, we propose a novel sampling-based method in the Bayesian filtering framework to address the problem. Within the framework, nearest neighbor field estimation is utilized to compute the importance proposal probabilities, which guide the Markov chain search towards promising regions and thus enhance the sampling efficiency; given the motion priors, a smoothing stochastic sampling Monte Carlo algorithm is proposed to approximate the posterior distribution through a smoothing weight-updating scheme. Moreover, to track the abrupt and the smooth motions simultaneously, we develop an abrupt-motion detection scheme which can discover the presence of abrupt motions during online tracking. Extensive experiments on challenging image sequences demonstrate the effectiveness and the robustness of our algorithm in handling the abrupt motions.

Keywords: Visual tracking, abrupt motion, stochastic sampling, nearest neighbor field, Markov Chain Monte Carlo

*Corresponding author. Present address: 5 South Zhongguancun Street, Haidian District, Beijing 100081, China.
Email address: vis_yl@bit.edu.cn (Yao Lu)

1. Introduction

Visual tracking can be viewed as a process of establishing temporal coherent relations between consecutive frames. Applications of visual tracking have been commonly found in surveillance [1, 2], human-computer interaction [3] and medical imaging [4], etc. Although great performance improvement has been achieved so far, the problem is still very challenging, especially in real-world scenarios that usually contain abrupt motions. Most existing approaches provide inferior performance when encountered abrupt motions because of their susceptibility to the motion discontinuity. In this work, we seek to develop an effective sampling-based algorithm to address the abrupt motion tracking problem.

Here, *abrupt motion* is defined as the sudden changes of an object's location. It may occur with various reasons: fast motion, shot changes, and low-frame-rate data source, etc. Fig. 1 illustrates some examples of the first two situations. Developing a robust tracking algorithm in such complex scenarios is rather challenging, and several problems need to be thoroughly resolved:

First, most existing approaches cannot capture the unexpected object dynamic. Particle filter(PF) has been demonstrated as a powerful method to deal with the non-Gaussian and the multi-modal state space for visual tracking (e.g., [5–12]). Although performing well in low-dimensional systems, these methods have to draw a large number of particles to guarantee sufficient sampling when abrupt motion occurs in which case the posterior density is very complex. The large computational cost makes PF infeasible for practical applications. Recently, Markov Chain Monte Carlo(MCMC) [13, 14] is widely used as an effective alternative of PF because of the high computational efficiency in high-dimensional sample space. However, it has been shown that MCMC-based tracking methods [15, 16] are prone to getting trapped in local modes when the energy landscape of the posterior distribution is rugged.

The second problem that has not been addressed by previous studies is tracking the abrupt and the smooth motions at the same time. In abrupt motion tracking, it is commonly assumed that the target almost moves smoothly but

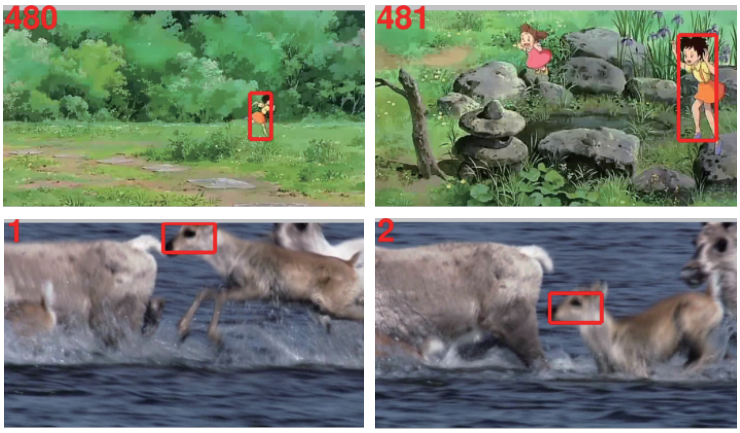

Figure 1: Examples of two abrupt motion scenarios. Top Row: *shot change*. Bottom Row: *Fast Motion*. Our tracking method successfully tracks the targets in these situations.

abruptly changes over several frames. However, most trackers [17, 18] simply consider all moves as abrupt changes and thus tend to suffer from drifting in case of background clutter or distractions.

To overcome these difficulties, we present a novel stochastic sampling method for abrupt motion tracking. First, we utilize an approximate nearest neighbor field (ANNF) algorithm to compute the importance proposal probabilities, which drive the Markov chain dynamics and achieve tremendous speedup in comparison with previous methods [17, 18]. Second, we incorporate the ANNF into a smoothing stochastic approximation Monte Carlo (SSAMC) framework. Within the framework, we consider that adjacent subregions probably bear similar likelihood to the target template, and accordingly develop a smoothing weight-updating step to distribute the information in each candidate to its neighborhood. The smoothing step not only improves the efficiency of the existing Monte Carlo algorithms, but makes our tracker robust to the noises in the nearest neighbor field. Furthermore, to track the abrupt and the smooth motions simultaneously, we develop an effective abrupt-motion detection scheme to discover the presence of sudden changes during tracking so that we can adjust

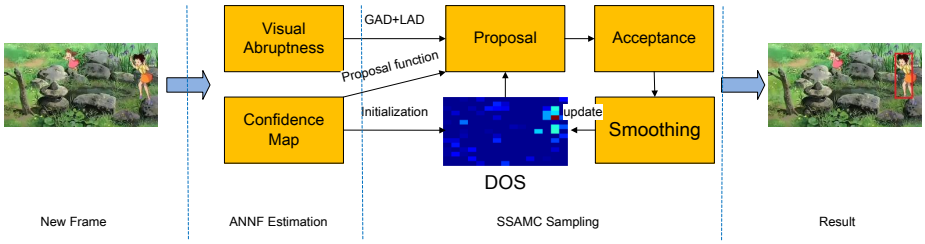

Figure 2: Flow chart of the proposed tracker. The confidence and the visual abruptness guide the sampling around the posterior modes, and the sampler iteratively updates the density-of-states to achieve good estimation.

the sample space for more efficient sampling. Fig. 2 illustrates an overview of our system, and Algorithm 1 describes our algorithm.

Note that the conference version of this work is presented in [19], and this article deepens and expands our previous work. In particular, 1) we present a substantial additional number of discussions and analysis about the previous literature on abrupt motion tracking; 2) we develop an abrupt-motion detection scheme to handle the challenging problem of tracking the abrupt and the smooth motions simultaneously; 3) we formalize the proposed stochastic sampling algorithm and bridge the gap between ANNF and the sampler using a weighted trial distribution; 4) we perform various additional experiments to evaluate the effectiveness of our algorithm for tracking.

The remainder of this paper is organized as follows: we review the related work in Section 2. In Section 3, we generalize the ANNF estimation into abrupt motion tracking, which is followed by the proposed sampling-based tracker in Section 4. The results of experiments and performance evaluation are shown in Section 5. Finally, we summarize our work with remarks on potential extensions in Section 6.

2. Related Work

There is a rich literature on visual tracking, and a full review of it is beyond the scope of this work (some are provided in [20, 21]). Here, we only discuss the

relevant work that motivated our paper.

Particle filter(PF) based methods [5–12] have been proven powerful in dealing with the non-Gaussian and the multi-modal state space for visual tracking. Many assume that the object in question moves smoothly between consecutive frames. Such a simplified assumption may work well in simple lab environment; however, it would have troubles in tracking the abrupt motions without significant drift in complex scenes. To address the limitations of PF, Michael *et al.*[22] incorporate the condensation algorithm into the importance sampling to track the target in high-dimensional sample space. Similarly, Vasanth *et al.*[23] combine PF with the quasi-random sampling to handle the abrupt changes. However, both methods are subject to the local-trap problem in abrupt motion tracking. Su *et al.*[24] incorporate a visual saliency model into the particle filtering framework. However, tracking failure will be caused by the background clutter because the saliency cannot be reliably estimated.

Traditional approaches for abrupt motion tracking are based on multi-scale representation [25], layered sampling [26] and multi-observation model [10]. Hua *et al.*[25] propose a multi-scale collaborative searching strategy based on the dynamic Markov network. Sullivan *et al.*[26] propose to combine observation likelihoods in different scales for accurate Bayesian estimation. Multi-scale methods can largely reduce the effect of the fast motion and the search space. However, the down-sampling operation may induce information loss to a certain extent. Therefore, in [10], multi-observation model is constructed on the same image space to alleviate the information loss. While this method shows promising results in face tracking, the off-line learning procedure makes it practically infeasible.

Our work is also related with approximate nearest neighbor field estimation [27–29]. This technique has found recent success in many computer vision areas, such as large displacement optical flow estimation [30, 31], and orderless tracking [32], etc. The ANNF estimation does not rely on the motion continuity; hence, it can provide relatively accurate motion information even though there are great changes.

More recently, the idea of using Markov Chain Monte Carlo in the sequential importance re-sampling particle filter has been widely explored [15–18, 33]. These approaches typically replace the importance sampling in particle filter with a MCMC sampling step, which is more efficient in high-dimensional spaces. Our work is partly motivated by the work [17, 18]. Kwon *et al.*[17] propose to utilize the Wang-Landau Monte Carlo(WLMC) sampling method to deal with the local-trap problem in abrupt motion tracking. Along with this thread, in Bayesian context, Zhou *et al.*[18] propose an intensively adaptive MCMC sampling method for abrupt motion tracking. Compared with [17], the posterior distribution can be more effectively estimated by a stochastic approximation process. However, this method has to explore the whole sample space uniformly with an inefficient preliminary sampling phase. Moreover, both two methods consider each move as an abrupt motion, which will cause the trackers' failure in cluttered scenes.

We make two main complementary improvements to [17, 18]. First, we propose a novel stochastic sampling method to search for the global optimum state in the large solution space. The nearest neighbor field is computed between consecutive frames to guide the Markov chain search and enhance the efficiency in stochastic sampling stage. Second, we leverage an abrupt-motion detection scheme to discover unexpected motions in a sequence so that our sampler can adjust the search space adaptively. This enables us to address the tracking problem including both abrupt and smooth motions.

3. Generalizing ANNF into Abrupt Motion Tracking

In this section, we discuss how to generalize the approximate nearest neighbor field estimation into abrupt motion tracking. A nearest neighbor field between two images is defined as: for each patch in an image, the most similar patch in another image. In this work, given two temporally adjacent frames at $t-1$ and t (assuming frame $t-1$ has been tracked), we discover the rough mode of the target in frame t using the patch matching method [28]. Additionally,

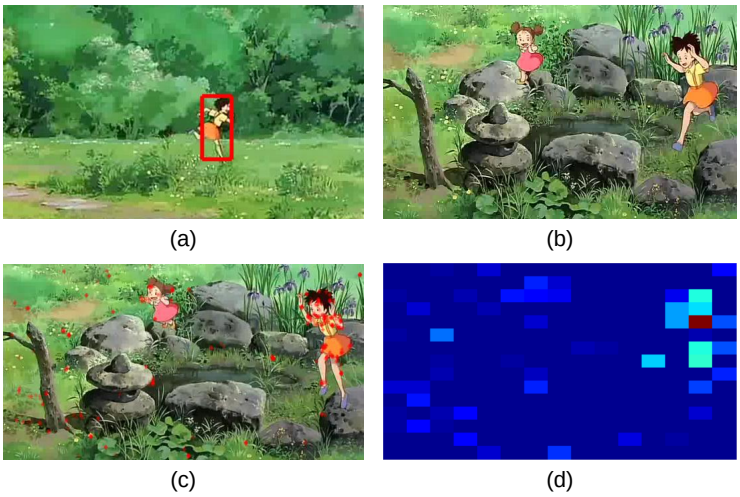

Figure 3: (a)(b)Abrupt motion with shot change; (c)Forward-backward matching result. Each red pixel indicates the center of a patch. (d) The confidence map which gives the rough regions that the target might be in.

the field enables us to determine whether abrupt motions occur in frame t.

Confidence Map Inspired by the occlusion reasoning scheme in [34], we employ a forward-backward consistency check of the correspondence to achieve more accurate field. In particular, let p_{t-1} denote the center of a patch within the bounding box in frame $t-1$, the forward matching patch in frame t is denoted as its center q_t; the backward matching patch corresponding to q_t is s_{t-1}. In this work, we assume that q_t is reliably estimated if the backward matching patch s_{t-1} belongs to the bounding box in frame $t-1$. By removing the unreliable correspondences, we obtain a set of patches $\mathcal{O}_t$ which are viewed as the promising regions where the target might be in the t-th frame. Then, the confidence of a pixel o in $\mathcal{O}_t$ is estimated according to its *incoherence*[28], which is defined as the pixel numbers M^o_{t-1} at time $t-1$ that o is mapped to, as computed by,

$$H^o_t = \begin{cases} M^o_{t-1} & \text{if} \quad o \in \mathcal{O}_t, \\ 0 & \text{otherwise} \end{cases} \tag{1}$$

where H_t^o is the incoherence of the pixel o at time t. Given the incoherence map, the confidence map (Fig. 3(d)) is obtained by a quantization process on m disjoint subregions (Section 4.4),

$$\lambda_t^i = \frac{\sum_{o=1}^{N_t^i} H_t^o}{N_t^i} \tag{2}$$

where λ_t^i is the confidence of the i-th subregion at time t and N_t^i indicates the pixel number in it.

Abrupt-motion Detection To make our algorithm robust in both abrupt and smooth scenarios, we propose two criteria which can well evaluate the abrupt degrees of the target and the background.

• *Global Abrupt Degree(GAD).* This criterion evaluates how much a frame has changed in comparison with previous frame. It is computed with the consideration that the matching error image represents the variance of the pixels between consecutive frames. However, we observe that the matching errors in high-frequency regions, e.g., the edges, are always large when using [28] which misleads the abrupt-degree estimation. Thus, we refine the error image Γ_t at time t using the edge map D_t to get a refined error image R_t,

$$R_t = \frac{\Gamma_t}{\mathrm{DIL}(D_t) + A} \tag{3}$$

where A is an all-one matrix and $\mathrm{DIL}(\cdot)$ denotes a dilation operator with a specific structuring element object, that is, a 3×3 all-one matrix. Then, the global degree g_t is computed by,

$$g_t = \frac{\sum_{i=1}^{U_t} R_t^i}{\max(R_t) \times U_t}, \quad \max(R_t) = \max(R_t^1, R_t^2, \ldots, R_t^{U_t}) \tag{4}$$

where U_t denotes the number of pixels in frame t, and R_t^i indicates the error value of the i-th pixel.

• *Local Abrupt Degree(LAD).* While the global abrupt degree is effective under camera switching conditions, it leads to unsatisfactory estimation results in other cases, e.g., fast motion. The limitation is overcome by the local measurement. Given the pixels $\boldsymbol{p}$ in the bounding box at time $t-1$ and the matching

set $\boldsymbol{q}$ at t, we model them with K-component Gaussian mixture model(GMM), respectively,

$$\Pr_{t-1}^{\boldsymbol{p}}(x) = \sum_{k=1}^{K} \pi_k \mathcal{N}(x|\mu_k, \Sigma_k), \quad \Pr_{t}^{\boldsymbol{q}}(x) = \sum_{k=1}^{K} \pi'_k \mathcal{N}(x|\mu'_k, \Sigma'_k) \tag{5}$$

where the k-th component in the sample distribution $\Pr_{t-1}^{\boldsymbol{p}}(x)$ is characterized by normal distribution $\mathcal{N}(x|\mu_k, \Sigma_k)$ with weight π_k, mean μ_k and covariance matrix Σ_k, and it is similar in $\Pr_{t}^{\boldsymbol{q}}(x)$. Note that the representation is supported by the theory that each single pixel can be presented in a distribution as a δ function which can be generally written as a Gaussian distribution with zero covariance. We now use the Hellinger distance[35] to compute the similarity between the two GMMs. Here, the distance is to measure the local abrupt degree l_t in the t-th frame,

$$l_t^2 = 1 - \int \sqrt{\Pr_{t-1}^{\boldsymbol{p}}(x) \times \Pr_{t}^{\boldsymbol{q}}(x)} dx \tag{6}$$

Given the global degree g_t and the local degree l_t, the abruptness V_t of the target can be computed by,

$$V_t = \begin{cases} 1 & \text{if} \quad g_t > T, \\ \text{sign}(a_t - 0.5) & \text{otherwise} \end{cases} \tag{7}$$

where T is empirically set to $[0.1, 0.2]$ and $a_t = 0.55 + g_t \times (l_t - 0.45)$. Here, frame t is considered as an abrupt frame if V_t equals to one.

Note that although the ANNF provides valuable prior information about the target's movements, a naïve embedding of the field into visual tracking requires the consideration of several factors, such as the noises in the field, the drifting problem due to short-term correspondence, etc. In this study, we use a smoothing stochastic sampling Monte Carlo algorithm (Section 4), which is robust to noise, to estimate the accurate state of the target from a noisy nearest neighbor field.

4. Stochastic Sampling Based Tracking Algorithm

4.1. Bayesian Formulation

In this work, visual tracking is formulated as a dynamic Bayesian inference task in hidden Markov model. Let $X_t = \{x_t, y_t, s_t\}$ represent the state of a target at time t, where (x_t, y_t) indicates the 2D coordinate of the target in the image plane, and s_t denotes its scale. Given the observations $Z_{1:t} = \{z_1, z_2, \cdots, z_t\}$ up to the t-th frame, we estimate the optimal state of the target at time t by the *maximum a posterior*(MAP) estimator:

$$\hat{X}_t = \underset{X_t^i}{\operatorname{argmax}}\, p(X_t^i|Z_{1:t}) \tag{8}$$

where X_t^i indicates the i-th sample at time t. According to the Bayes theorem, the posterior distribution $p(X_t|Z_{1:t})$ can be estimated recursively by:

$$p(X_t|Z_{1:t}) \propto p(Z_t|X_t) \int p(X_t|X_{t-1}) p(X_{t-1}|Z_{1:t-1}) dX_{t-1} \tag{9}$$

where $p(X_t|X_{t-1})$ is the motion model that describes the evolution of the state variable, and $p(Z_t|X_t)$ is the observation model measuring the similarity between the candidate samples and the appearance model.

4.2. Sampling

Directly sampling from the filtering distribution $p(X_t|Z_{1:t})$ is intractable since it is not a simple, standard distribution considered so far. However, as is often the case, we are able to evaluate the desired distribution for any given sample up to the normalizing constant $\mathcal{Z}_p$. Without loss of generality, in this sub-section, we use $p(x)$ to represent the filtering distribution for convenience. Then, we can write the distribution in the following form:

$$p(x) = \frac{1}{\mathcal{Z}_p} \tilde{p}(x),\ x \in \mathcal{X} \tag{10}$$

where the density $\tilde{p}(x)$ gives the unnormalized probability of a state, and can be readily evaluated; $\mathcal{X}$ indicates the sample space. In physics and chemistry, $\tilde{p}(x)$ is commonly called the Boltzmann factor:

$$\tilde{p}(x) = \exp(-E(x)),\ x \in \mathcal{X} \tag{11}$$

Algorithm 1 The proposed abrupt motion tracking algorithm.

Input: Image frames $F_1, F_2, \cdots, F_T$; object state $\hat{X}_1$ in the first frame; iteration number K; sample number N in each iteration.
Output: Tracking results $\{X_t\}_{t=2}^{T}$.
Initialize:
  Foreground and background HSV histograms generation: h_F and h_B
  Image space partition: $\mathcal{X} = \bigcup_{i=1}^{m} E_i$
Main Procedure:
for $t = 1$ to T **do**
  //ANNF Stage
  Estimate the confidence map λ_t using Eq. (2);
  Detect the presence of abrupt motions according to Eq. (7).
  //SSAMC Stage
  Determine the sample space $\mathcal{X}'_t$ according to Eq. (17);
  for $k = 1$ to K **do**
    for $n = 1$ to N **do**
      (*Proposal*) Propose a candidate sample X'_t using Eq. (15);
      (*Acceptance*) Accept X'_t with probability α in Eq. (18);
    end for
    (*Smoothing*) Calculate $\mathbf{f}^k = (f_1^k, f_2^k, \ldots, f_m^k)$ in Eq. (20);
    Update the density-of-states according to Eq. (22);
  end for
  //Inference
  MAP estimate to get $\hat{X}_t$.
end for

where $E(x)$ is an energy function.

4.3. Metropolis-Hastings Algorithm

The Metropolis-Hastings algorithm is now widely used to estimate the filtering distribution because it can draw samples from probability distribution $p(x)$, if we can easily evaluate the value of $\tilde{p}(x)$. Note that it is not necessary to calculate $\mathcal{Z}_p$ which is often difficult in practice. As more samples are proposed, the distribution of these samples more closely approximates the desired distribution $p(x)$. The algorithm is performed in two steps:

- **Proposal Step** Draw a candidate state X_t' from a proposal function $Q(X_t'|X_t)$ given the current state X_t. The function Q is commonly designed based on a motion transition model, e.g., the Gaussian distribution.

- **Acceptance Step** Compute the acceptance probability α, which is used to determine whether to accept or reject the candidate:

$$\alpha(X_t'; X_t) = \min\{1, \frac{p(X_t'|Z_{1:t})Q(X_t; X_t'))}{p(X_t|Z_{1:t})Q(X_t'; X_t))}\} \tag{12}$$

While the Metropolis-Hastings based tracking algorithms[2, 16] work well in some cases, it is prone to get trapped in the local energy maxima when the energy landscape of the state space is rugged. In the next section, we introduce a novel stochastic sampling method to alleviate this problem.

4.4. Abrupt Motion Tracking via Stochastic Sampling

As discussed in Section 4.2, the Boltzmann distribution can help predict the probability distribution for the energy function E. However, once the abrupt motions occur, the energy landscape will be rugged, and this will cause the local-trap problem. To address this issue, we partition the image space $\mathcal{X}_t$ at time t into m disjoint subregions $\mathcal{X}_t = \bigcup_{i=1}^{m} E_i$ according to the energy function $E(x)$. Here, $E(x) = p(X_t|Z_{1:t})$ is the posterior probability in Eq. (9). Then, we design an effective sampler to simulate a random walk in the subregions so that the motion uncertainty can be captured.

Instead of the original posterior distribution, we construct a novel trial density function, called weighted trial function, for importance sampling,

$$p_\omega(X_t) \propto \sum_{i=1}^{m} \lambda_t^i \frac{p(X_t|Z_{1:t})}{\omega_i} I(X_t \in E_i) \tag{13}$$

where λ_t^i is the confidence of the i-th subregion at time t, which controls the sampling frequency of this subregion; $I(\cdot)$ is the indicator function, and $\omega_i = \int_{E_i} p(X_t|Z_{1:t})dX_t$ is called density-of-states (DOS) of the distribution. It has been demonstrated that if we are able to estimate the density term for each subregion, sampling from $p_\omega(X_t)$ will lead to a random walk in the image space (by regarding each subregion as a point) [36]. Hence, the local-trap problem can be overcome. Compared with [18], the weight parameter λ_t^i in the trial distribution controls the similarity between the target distribution, i.e., $p(X_t|Z_{1:t})$ and the trial distribution $p_\omega(X_t)$. Clearly, one can incorporate any priors into the trial function by adjusting the weight parameter. Here, the ANNF is utilized to conduct the sampler to coverage fast to the posterior distribution.

In what follows, we elaborate the three major stages in our sampling-based tracking algorithm, which are, the proposal step, the acceptance step and the smoothing step.

4.4.1. Proposal Step

The choice of the proposal function is significant to our algorithm. For continuous sample space, a common choice is the Gaussian distribution centered on the current state, leading to an important trade-off in determining the variance of this proposal function. [17, 18] use a large variance to capture large motions, in which case, a large percentage of samples are drawn from the unpromising regions, thereby decreasing the acceptance rate. In this work, we observe that the states with high posterior probability should be more frequently sampled, and vice versa. Therefore, we develop an adaptive proposal function based upon the ANNF estimation (Section 3). The field provides importance probabilities for the image subregions to make the samples in promising regions be proposed with higher probabilities.

Our proposal function includes two basic moves: *global random walk* and *local random walk*. Notably, 1) we perform global random walk on the image subregions $\mathcal{X}_t$ to account for the large motion uncertainty. At each move, a subregion E_i will be selected with probability ρ,

$$\rho(E_i) = \begin{cases} \theta & \text{if} \quad \lambda_t^i > 0, \\ 1-\theta & \text{otherwise} \end{cases} \tag{14}$$

where $\rho(E_i) = \theta$ if E_i contains at least one patch in the ANNF of frame t. After selecting a subregion, a candidate pixel is uniformly determined within it; 2) we also perform a Gaussian random walk to explore the local sample space whose step size varies according to the normal distribution. The local random walk tends to propose the states close to the previous one since the target generally moves smoothly.

With the aforementioned notations, our proposal distribution can be formulated into a mixture model,

$$Q(X_t'; X_t) = \beta \mathcal{N}(X_t'; X_t, \Sigma) + (1-\beta) Q_a(X_t'; X_t) \tag{15}$$

where $\mathcal{N}(\cdot; X_t, \Sigma)$ is a normal distribution with mean $\mu = X_t$ and a small variance Σ; $Q_a(X_t'; X_t)$ is an adaptive proposal function,

$$Q_a(X_t'; X_t) \propto \rho(E_j), \quad \text{where} \quad X_t' \in E_j \tag{16}$$

The parameter $\beta \in [0, 1]$ in Eq. (15) balances the proposal between the global random walk and the local random walk.

To track the abrupt and the smooth motions simultaneously, our proposal function adaptively adjusts the candidate sample space $\mathcal{X}_t'$ according to the abruptness of the frame,

$$\mathcal{X}_t' = \begin{cases} \mathcal{L}(\hat{X}_{t-1}) & \text{if} \quad V_t = 0, \\ \mathcal{X}_t & \text{otherwise} \end{cases} \tag{17}$$

where $\hat{X}_{t-1}$ denotes the best state in previous frame, and $\mathcal{L}(\cdot)$ indicates the nearby regions of a state, e.g., 5×5 neighborhood. Note that this adaptive

proposal always biases the sampling towards the promising regions to improve the sampling efficiency as well as the accuracy of the state estimation.

4.4.2. Acceptance Step

Suppose that a candidate sample X_t' has been generated using the proposal function in Eq. (15), accepting it or not is determined by the Metropolis-Hastings rule,

$$\begin{aligned}\alpha(X_t'; X_t) &= \min\left\{1, \frac{p_\omega(X_t')}{p_\omega(X_t)}\frac{Q(X_t; X_t')}{Q(X'; X_t)}\right\} \\ &= \min\left\{1, \frac{P(X_t'|Z_{1:t})\frac{\lambda_t^{J_{X_t'}}}{\omega_{J_{X_t'}}}Q(X_t; X_t')}{P(X_t|Z_{1:t})\frac{\lambda_t^{J_{X_t}}}{\omega_{J_{X_t}}}Q(X_t'; X_t)}\right\}\end{aligned} \tag{18}$$

where J_{X_t} denotes the index of the subregion containing X_t. Different from [17, 18], the density of each subregion is initialized with its confidence,

$$\omega_i = \exp(-\tau \times \lambda_t^i) \tag{19}$$

where τ is empirically set to 1000 in our experiments.

Our acceptance ratio in (18) has two advantages compared to that in [17, 18]. The first is that the acceptance ratio and the density initialization procedure enable us to escape from the local maxima and reach the global maximum. At a local maximum, the ratio $\frac{\lambda_t^i}{\omega_i}$ initially has a larger value than that at the global maximum because the confidence value λ_t^i is smaller, and the DOS term ω_i is larger according to (19). Hence, the samples at the local maximum are more easily rejected compared with those at the global maximum. While the simulation goes on, the ratio will further decrease because the DOS will increase(Section 4.4.3). By contrast, the ratio at the global maximum will increase. This process helps our algorithm escaping the local maxima; second, during tracking, the confidence value λ_t^i in (18) always drives our sampler to accept the candidate samples in the promising regions. This largely reduces the rejection rate and enhances the sampling efficiency.

4.4.3. Smoothing Step

The success of stochastic approximation Monte Carlo(SAMC) algorithm [36] depends crucially on the self-adjusting mechanism, which enables the sampler to explore the entire image space. However, the density learning method in SAMC has not yet reached the maximal efficiency since it ignores the difference between the neighboring and the non-neighboring regions. Intuitively, a sample X_t may contain some information of the neighboring regions. For instance, if X_t in subregion E_i is rejected, the samples in the neighborhood will be probably rejected as well, and vice versa. Accordingly, we improve the density learning method by including a smoothing step at each iteration.

More specifically, in the proposal step, we allow multiple samples to be generated at each iteration and employ a smoothed estimator f_i^k when updating the density-of-state term, where f_i^k is the probability that a sample can be drawn from the subregion E_i at iteration k. Let $X_t^{(k,1)}, X_t^{(k,2)}, \ldots, X_t^{(k,n)}$ be n samples generated in the proposal step at iteration k in frame t. Since n is usually a small number($n = 5$ in our experiment), the samples form a sparse frequency vector $\mathbf{r}^k = (r_1^k, r_2^k, \ldots, r_m^k)$ with $r_i^k = \sum_{j=1}^n I(X_t^{(k,j)} \in E_i)$. It is worth mentioning that r_i^k/n is not a good estimation for f_i^k because the law of large numbers does not serve in this situation. Since the image space is partitioned smoothly in this paper, we assume that information in nearby regions can help produce more accurate estimate of f_i^k. Therefore, we improve the frequency estimator with a smoothing method, that is, the Nadaraya-Waston kernel estimator [37],

$$f_i^k = \frac{\sum_{j=1}^m W(M(i-j)) r_j^k/n}{\sum_{j=1}^m W(M(i-j))} \tag{20}$$

where $M(i-j)$ measures the Euclidean distance between the centers of subregions E_i and E_j. $W(\cdot)$ is a double-truncated Gaussian kernel function to control the smoothing scope,

$$W(z) = \begin{cases} \exp(-z^2/2) & \text{if} \quad |z| < C, \\ 0 & \text{otherwise} \end{cases} \tag{21}$$

where C is empirically set to 100. After achieving the smoothed estimation

$\mathbf{f}^k = (f_1^k, f_2^k, \ldots, f_m^k)$, we update the density-of-state of E_i as,

$$\omega_i^{k+1} = \omega_i^k + \exp(\gamma_k(f_i^k - \pi_i)), \quad i = 1, 2, \ldots, m \tag{22}$$

where ω_i^k indicates the DOS term of E_i at iteration k; $\pi = (\pi_1, \pi_2, \ldots, \pi_m)$ is a vector with $0 < \pi_i < 1$ and $\sum_{i=1}^m \pi_i = 1$, which defines the desired sampling frequency of each subregion; $\gamma_k = \frac{k_0}{\max(k_0,k)}$($k_0$ is a pre-specified constant) is a gain factor controlling the updating speed of the density-of-states.

The smoothing weight-updating step has more superiorities in comparison to the existing algorithms: 1) suppose a candidate is rejected in the acceptance step, the density-of-states of the subregions that the candidate belongs to and nears with will be adjusted to a larger value. Thus, in the next iteration, our algorithm can jump out from these subregions with a high probability. This is important for our approach not to fall into the local maxima; 2) by distributing the information contained in a subregion to the nearby ones, the smoothing scheme in the weight-updating step not only improves the accuracy of the DOS estimation, but makes our method robust to the noises in the ANNF.

5. Experimental Results

5.1. Experiment Setup

The proposed tracker is implemented in MATLAB and runs at 2fps on a PC. Given an image sequence, we manually label the state of the target in the first frame. For brevity, we will refer our method as SSAMC from now on.

In this work, we utilize the color-based appearance model [5]. The foreground and the background are represented with two HSV histograms h_F and h_B, respectively. The number of bins in each channel is equally set to 10. For each candidate X_t^k, we estimate the similarity between the state and the templates with Bhattacharyya metric, $d_F = D(X_t^k, h_F)$ and $d_B = D(X_t^k, h_B)$. Finally, the likelihood function is formulated as $p(Z_{1:t}|X_t^k) = \frac{1}{1+\exp(d_F - d_B)}$.

In our experiments, we set the patch size to 8×8 for the ANNF estimation. The image space is empirically partitioned into 15×15 disjoint subregions

Table 1: The sequences and their challenges

Sequence	Main Challenge	Length
Animal	Fast Motion	15
Tennis	Fast Motion	31
Boxing	Shot Change	813
Youngki	Shot Change	770
Badminton	Fast Motion & Occlusion	281
Pingpong	Fast Motion & Occlusion	139

according to the energy function E_x. The proposal variance in Eq. (15) is set to $\Sigma = diag(\sigma_x^2, \sigma_y^2, \sigma_s^2) = diag(8.0^2, 4.0^2, 0.013^2)$ in which σ_x and σ_y denote the variances of 2D coordinate, and σ_s denotes the variance of target scale. In Eq. (14), θ is empirically set to 0.8. β in Eq. (15) is set to 0.2 to facilitate the global exploration of the proposal function. k_0 in the gain factor is set to $N/4$ where N is the number of samples. In every experiment, the iteration number K for sampling is 120 and in each iteration, we propose $n = 5$ samples. The desired sampling distribution is set to be uniform, e.g., $\pi_i = 1/m, i = 1, 2, \ldots, m$. For fair evaluation, in Eq. (7), we fix the parameter $T = 0.2$ in our experiments, although slightly different values for different videos can produce better results.

To evaluate our algorithm, we selected 6 typical image sequences with various abrupt motion properties from [17]. Details about the sequences are listed in Tab. 1. We compare the proposed method with other 6 state-of-the-art algorithms: WLMC [17], SAMC [18], SCM [9], VTD [38], LSST [7], and saliency-based particle filter (referred as SaPF) [24]. For fair comparison, we run the source codes provided by the authors with tuned parameters to obtain their best performance.

5.2. Quantitative Evaluation

1) *Performance of the Tracking Algorithms:* Two widely used criteria have been employed in this paper to evaluate the performance of the trackers: 1) *Cen-*

Table 2: Average center location error(in pixel). The best and second best results are shown in red and blue fonts.

	LSST	SCM	VTD	SaPF	WLMC	SAMC	SSAMC
Animal	107.59	54.17	124.30	100.69	49.70	17.94	**17.51**
Tennis	75.83	105.09	102.79	45.24	36.12	19.91	**7.01**
Boxing	127.72	60.62	74.92	14.52	14.08	13.00	**12.49**
Youngki	83.74	130.36	73.55	26.94	17.52	**12.74**	14.99
Badminton	53.82	50.59	32.76	34.12	46.13	44.81	**23.99**
Pingpong	73.12	74.27	45.77	54.15	179.95	56.12	**30.31**
Average	86.97	79.18	75.68	45.94	57.25	27.42	**17.72**

Table 3: Average overlap rate. The best and second best results are shown in red and blue fonts.

	LSST	SCM	VTD	SaPF	WLMC	SAMC	SSAMC
Animal	0.04	0.37	0.05	0.12	0.35	0.65	**0.72**
Tennis	0.05	0.27	0.06	0.48	0.46	0.66	**0.79**
Boxing	0.12	0.38	0.34	0.75	0.78	**0.79**	0.78
Youngki	0.34	0.21	0.42	0.70	0.77	**0.83**	0.82
Badminton	0.37	0.38	0.50	0.46	0.34	0.43	**0.68**
Pingpong	0.32	0.30	0.42	0.33	0.08	0.36	**0.47**
Average	0.21	0.32	0.30	0.47	0.46	0.62	**0.71**

ter Location Error(CLE) that evaluates the position errors between the centers of the tracking results and those of the ground truth; 2) *VOC Overlap Ratio(VOR)* that measures the success ratio of the algorithms, which is calculated by $VOR = \frac{|B_r \cap B_g|}{|B_r \cup B_g|}$, where B_r denotes the tracked bounding box, B_g is the ground truth box and $|\cdot|$ denotes the number of pixels in a region. Besides, the average CLE and the average VOR are calculated on each sequence to evaluate the overall performance of our tracker.

Table 4: Average center location error(in pixel) when there are only smooth motions. The best and second best results are shown in red and blue fonts.

	LSST	SCM	VTD	SaPF	WLMC	SAMC	SSAMC
Boxing	17.23	12.80	12.95	14.33	13.19	12.81	**12.49**
Youngki	19.01	15.02	13.22	24.40	17.35	**12.63**	14.99
Badminton	53.82	50.59	32.76	34.12	46.13	44.81	**23.99**
Pingpong	73.12	74.27	45.77	54.15	179.95	56.12	**30.31**

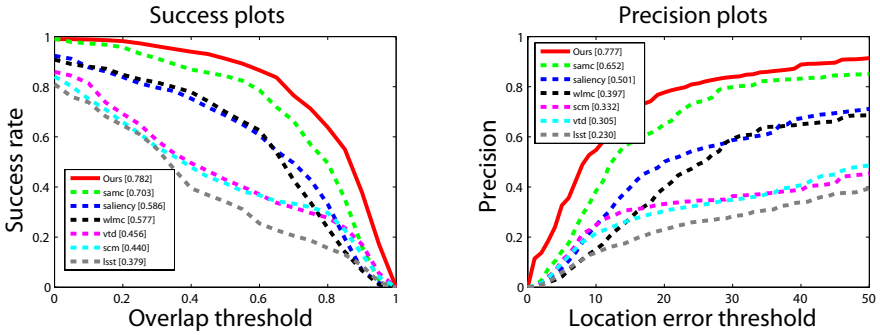

Figure 4: Precision Plots and Success Plots. The overall performance score for each tracker is shown in the legend.

Tab. 2 and Tab. 3 respectively summarize the average CLE and the average VOR of all the six trackers on all 6 sequences. The potential benefits of our tracker are notable: it performs best on 5 of 6 videos in terms of the average CLE, and 4 of 6 videos in terms of the average VOR. Besides, it outperforms other trackers by the smallest average CLE and the largest average VOR over all the image sequences. The performance improvement is particularly impressive in the *Animal*, *Tennis*, *Badminton* and *Pingpong* sequences. In the *Animal* and *Tennis* sequence, the targets move rapidly with unpredictable directions and distances. Our tracker benefits greatly from the approximate nearest neighbor field that makes the samples be drawn from the promising regions. Besides, the sequences *Badminton* and *Pingpong* mainly consist of smooth motions. In

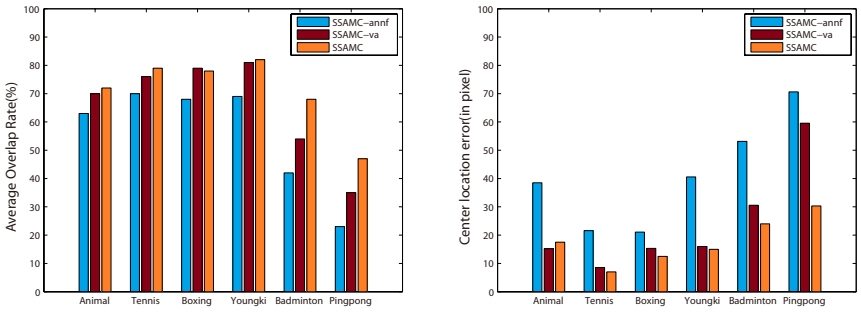

Figure 5: Overlap rates(%) and location errors(in pixel) of SSAMC-annf, SSAMC-va and SSAMC on the sequences.

this situation, our tracker is more flexible because of the abrupt-motin detection scheme, while in [17] and [18], the large sampling variance causes severely tracking accuracy decrease of the smooth motions. In sum, our tracker outperforms other trackers on most sequences, although it shows slightly poor performance on *Boxing*(in terms of VOR) and *Youngki*. We attribute this to the fact that we have not considered scale changes of the target in this article; therefore the overlap rate will be a little inaccurate when the scale of the target frequently changes in *Boxing* and *Youngki*.

We further employ the Precision Plot and the Success Plot [39] to evaluate the overall performance of these algorithms, as illustrated in Fig. 4. The precision plot summarizes the percentage of frames whose tracking location is within a given distance R of the ground truth, and the success plot presents the ratios of successful frames at the thresholds in $[0, 1]$. Here, the successful frame is defined as the frame whose overlap value is larger than a given threshold τ(e.g., 90%). Obviously, our algorithm performs better than other trackers. More precisely, in the precision plots, it outperforms SAMC by **12.5%**, SaPF by **27.6%** and WLMC by **38.0%**, while in the success plots, it outperforms them by **7.9%**, **19.6%** and **20.5%**, respectively. Note that the numerical results are computed with the same scheme as [39]: the error threshold R is set to 20 pixels for ranking in the precision plots; while in the success plots, the area under

curve is utilized to rank the tracking algorithms.

The above-mentioned results show the great ability of our algorithm to track the abrupt and the smooth motions simultaneously. To further evaluate the performance of our tracker in handling the smooth motions, we compare it with other algorithms on *Boxing*, *Youngki*, *Pingpong* and *Badminton* movies. To only have smooth motions in sequences *Boxing* and *Youngki*, we reinitialized the states of other tracking approaches to the ground truth when the abrupt motions occur. The other two sequences remain unchanged. As listed in Tab. 4, the proposed algorithm outperforms other algorithms on these sequences even though we did not reinitialize its states. This demonstrates the effectiveness of our method in handling smooth motions.

2) *Performance of Abrupt-motion Detection:* To justify the effectiveness of the abrupt-motion detection in our algorithm, we construct a new tracker, the SSAMC-va tracker, in which the detection process of abrupt motions is neglected. Thus, the sample space $\mathcal{X}'$ in Eq. (14) is always $\mathcal{X}$, that is, the entire image space. The quantitative results are illustrated in Fig. 5. SSAMC-va shows worse performance than SSAMC on these sequences, especially on the sequences *Badminton* and *Pingpong*. The fundamental reason is that the abrupt-motion detection scheme largely improves the accuracy of SSAMC in the smooth motions while the SSAMC-va tracker easily drifts from the target in the smooth movements due to the background clutter. Therefore, the abrupt-motion detection method is important to our algorithm, especially in the scenarios with plenty of smooth motions and background clutter.

3) *Performance of ANNF Estimation:* To verify the effectiveness of the approximate nearest neighbor field estimation, we also construct a tracker called SSAMC-annf, in which no initial motion information is provided to the sampler. The density-of-states in the sampling stage are initialized with all one and the proposal probability for each cell is equally set to $1/m$ where m is the number of cells. The quantitative results in Fig. 5 prove the importance of ANNF because SSAMC, with ANNF estimation, shows much better performance than SSAMC-annf.

Table 5: Time Cost of the tracking methods

	WLMC	SAMC	SSAMC
Cost	2.4fps	4fps	2fps
Language	C/C++	C/C++	MATLAB

4) *Computational Cost:* We compare the computational cost of the proposed algorithm with other two sampling-based methods, WLMC [17] and SAMC [18]. The results, as shown in Tab. 5, are estimated under 640×480 videos and 600 samples. Note that our runtime is slightly longer than other algorithms mainly because we implement the algorithm in MATLAB language rather than C/C++. Taking this language factor into account, the proposed tracking algorithm has no additive computational burden compared to the other two methods, because the ANNF helps largely reduce the search space. Besides, the smoothing weight-updating scheme improves the convergence rate of the Markov chain.

5.3. Qualitative Evaluation

In this paper, we categorize the abrupt motions into two classes: *fast motion* and *Shot change*.

1) *Fast Motion:* We firstly evaluate these trackers on four challenging sequences with fast motion, which are *Animal*, *Tennis*,*Badminton* and *Pingpong*. The results are illustrated in Fig. 6. The *Animal* sequence is challenging for tracking as the target moves very fast. We can see that LSST, SCM, VTD, SaPF and WLMC methods drift from the beginning of the sequence(e.g., #5). The former three methods lost the target because they heavily depend on the motion continuity; as for SaPF, it is difficult to estimate accurate saliency map for the head of the animal; The WLMC tracker requires more samples (more than 1000) to track the target accurately, thus fails in this case. The SAMC and our method can track the targets successfully through the whole sequence.

In *Tennis* sequence, there are very fast motions and large pose changes of the player. LSST, SCM, VTD and SaPF trackers fail when the player moves

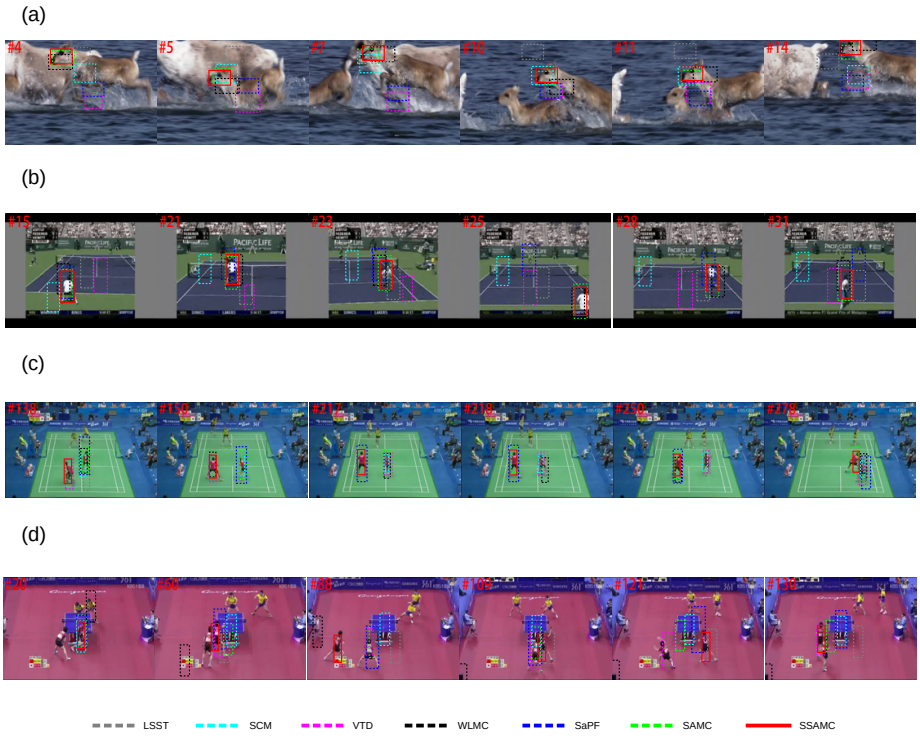

Figure 6: Tracking results on fast motion sequences: (a) *Animal*, (b) *Tennis*, (c) *Badminton*, (d) *Pingpong*. Figure best viewed in color.

back and forth. The WLMC tracker is slightly better, but still drifts in several frames (e.g., #23, #28). In contrast, SAMC and our trackers are able to track the player throughout the sequence. As shown in Tab. 2, our tracker is much better than other trackers in terms of the center location error.

In *Badminton* sequence, the object undergoes heavy occlusion in cluttered background, as well as fast motion in some frames. Most trackers drift away from the targets because of the interference of similar object in the background. As shown in Tab. 2 and Tab. 3, our method is better than others mainly because of the ANNF estimation and the background information included in the appearance model. The VTD method also performs well with relatively high overlap rates and low center location errors.

In the *Pingpong* sequence, most trackers drift due to the severe occlusion and

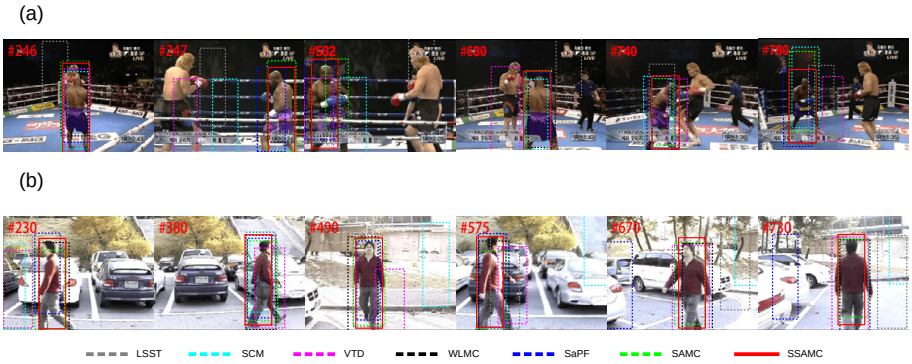

Figure 7: Tracking results on shot change sequences: (a) *Boxing* and (b) *Youngki*. Figure best viewed in color.

background clutters(e.g., #88, #130). Tracking such an object is extremely challenging because the two red players are difficult to distinguish, even for humans. As listed in Tab. 2 and Tab. 3, VTD and our method show significant better performance than other trackers. WLMC has the lowest overlap rate and the highest location error in this sequence because it drifts at the beginning due to background clutter(e.g., #20).

2) *Shot Change:* Fig. 7 shows the tracking results from two challenging sequences to evaluate that whether our method can tackle shot changes or not. In the *Boxing* sequence, the target moves smoothly at most time, but the position abruptly changes due to the camera switching. We can see that LSST, SCM and VTD trackers get lost in tracking the target after the shot changes(e.g., #247). In contrast, the SaPF, WLMC, SAMC and our approach achieve stable performance on the entire sequence.

In the sequence *Youngki*, a walker undergoes abrupt motions caused by sudden shot changes. The LSST, SCM and VTD trackers lose the target quickly(e.g., #230) since they can not capture the large motion uncertainty. SaPF eventually drift in this long-time sequences(e.g., #670). The WLMC, SAMC and our method track the objects throughout the sequence because the stochastic sampling scheme help to explore the sample space effectively to cap-

ture this type of motions. The proposed method is slightly worse than SAMC in terms of overlap rates and location errors, however, overall, our results remain acceptable.

6. Conclusion and Future Work

We have proposed a novel stochastic sampling method for abrupt motion tracking in the Bayesian filtering framework. Within the framework, the approximate nearest neighbor field estimation is utilized to discover the rough mode of the target at each frame; after incorporating it into the smoothing stochastic sampling Monte Carlo approach, our algorithm can more accurately estimate the state of the target. Moreover, we have developed an abrupt-motion detection scheme so that our tracker can effectively handle both abrupt and smooth motions. Experiments over several challenging sequences demonstrate the effectiveness of our method compared with other related methods.

In future work, we shall extend the proposed tracking algorithm in three directions: 1) we will firstly improve the method using a robust appearance model (e.g., [9, 11, 40]); 2) we aim to extend our algorithm to a more efficient one in order to address the abrupt changes in both position and scale; 3) finally, we will expand the method to track the abrupt motions in multi-target scenarios. Compared with [17, 18], our algorithm can achieve tremendous speedup because the motion fields for all targets can be estimated in a single run. We will further work on designing an effective data association method to track interactive objects.

Acknowledgements

We are thankful for the anonymous reviewers for their suggestions helping us to improve this work. We also acknowledge the support of the National Natural Science Foundation of China (No. 61273273) and by Research Fund for the Doctoral Program of Higher Education of China (No. 20121101110034).

References

[1] C. Stauffer, W. E. L. Grimson, Learning patterns of activity using real-time tracking, IEEE Transactions on Pattern Recognition and Machine Intelligence (TPAMI) 22 (2000) 747–757.

[2] B. Benfold, I. Reid, Stable multi-target tracking in real-time surveillance video, in: IEEE Conference on Computer Vision and Pattern Recognition (CVPR), IEEE, 2011, pp. 3457–3464.

[3] M. Kim, S. Kumar, V. Pavlovic, H. Rowley, Face tracking and recognition with visual constraints in real-world videos, in: IEEE Conference on Computer Vision and Pattern Recognition (CVPR), IEEE, 2008, pp. 1–8.

[4] N. Paragios, A level set approach for shape-driven segmentation and tracking of the left ventricle, IEEE Transactions on Medical Imaging 22 (2003) 773–776.

[5] P. Pérez, C. Hue, J. Vermaak, M. Gangnet, Color-based probabilistic tracking, in: European Conference on Computer Vision (ECCV), Springer, 2002, pp. 661–675.

[6] K. Nummiaro, E. Koller-Meier, L. Van Gool, An adaptive color-based particle filter, Image and vision computing 21 (2003) 99–110.

[7] D. Wang, H. Lu, M.-H. Yang, Least soft-threshold squares tracking, in: IEEE Conference on Computer Vision and Pattern Recognition (CVPR), IEEE, 2013, pp. 2371–2378.

[8] L. Cehovin, M. Kristan, A. Leonardis, An adaptive coupled-layer visual model for robust visual tracking, in: International Conference on Computer Vision (ICCV), IEEE, 2011, pp. 1363–1370.

[9] W. Zhong, H. Lu, M.-H. Yang, Robust Object Tracking via Sparse Collaborative Appearance Model, IEEE Transactions on Image Processing (TIP) (2014) 2356–68.

[10] Y. Li, H. Ai, T. Yamashita, S. Lao, M. Kawade, Tracking in low frame rate video: A cascade particle filter with discriminative observers of different lifespans, in: IEEE Conference on Computer Vision and Pattern Recognition (CVPR), IEEE, 2007, pp. 1–8.

[11] X. Jia, H. Lu, M.-H. Yang, Visual tracking via adaptive structural local sparse appearance model, in: IEEE Conference on Computer Vision and Pattern Recognition (CVPR), IEEE, 2012, pp. 1822–1829.

[12] J. Dou, J. Li, Robust visual tracking based on interactive multiple model particle filter by integrating multiple cues, Neurocomputing 135 (2014) 118–129.

[13] W. R. Gilks, Markov chain monte carlo, Wiley Online Library, 2005.

[14] F. Septier, S. K. Pang, A. Carmi, S. Godsill, On mcmc-based particle methods for bayesian filtering: Application to multitarget tracking, in: IEEE International Workshop on Computational Advances in Multi-Sensor Adaptive Processing (CAMSAP), IEEE, 2009, pp. 360–363.

[15] Z. Khan, T. Balch, F. Dellaert, An mcmc-based particle filter for tracking multiple interacting targets, in: European Conference on Computer Vision (ECCV), Springer, 2004, pp. 279–290.

[16] Z. Khan, T. Balch, F. Dellaert, Mcmc-based particle filtering for tracking a variable number of interacting targets, IEEE Transactions on Pattern Recognition and Machine Intelligence (TPAMI) 27 (2005) 1805–1819.

[17] J. Kwon, K. M. Lee, Wang-landau monte carlo-based tracking methods for abrupt motions, IEEE Transactions on Pattern Recognition and Machine Intelligence (TPAMI) 35 (2013) 1011–1024.

[18] X. Zhou, Y. Lu, J. Lu, J. Zhou, Abrupt motion tracking via intensively adaptive markov-chain monte carlo sampling, IEEE Transactions on Image Processing (TIP) 21 (2012) 789–801.

[19] T. Zhou, Y. Lu, H. Di, Nearest neighbor field driven stochastic sampling for abrupt motion tracking, in: IEEE International Conference on Multimedia and Expo (ICME), IEEE, 2014, pp. 1–6.

[20] A. Yilmaz, O. Javed, M. Shah, Object tracking: A survey, Acm computing surveys (CSUR) 38 (2006) 13.

[21] H. Yang, L. Shao, F. Zheng, L. Wang, Z. Song, Recent advances and trends in visual tracking: A review, Neurocomputing 74 (2011) 3823–3831.

[22] M. Isard, A. Blake, Condensation–conditional density propagation for visual tracking, International Journal on Computer Vision (IJCV) 29 (1998) 5–28.

[23] V. Philomin, R. Duraiswami, L. S. Davis, Quasi-random sampling for condensation, in: European Conference on Computer Vision (ECCV), Springer, 2000, pp. 134–149.

[24] Y. Su, Q. Zhao, L. Zhao, D. Gu, Abrupt motion tracking using a visual saliency embedded particle filter, Pattern Recognition 47 (2014) 1826–1834.

[25] G. Hua, Y. Wu, Multi-scale visual tracking by sequential belief propagation, in: IEEE Conference on Computer Vision and Pattern Recognition (CVPR), volume 1, IEEE, 2004, pp. I–826.

[26] J. Sullivan, A. Blake, M. Isard, J. MacCormick, Object localization by bayesian correlation, in: International Conference on Computer Vision (ICCV), volume 2, IEEE, 1999, pp. 1068–1075.

[27] C. Barnes, E. Shechtman, A. Finkelstein, D. Goldman, Patchmatch: a randomized correspondence algorithm for structural image editing, ACM Transactions on Graphics-TOG 28 (2009) 24.

[28] S. Korman, S. Avidan, Coherency sensitive hashing, in: International Conference on Computer Vision (ICCV), IEEE, 2011, pp. 1607–1614.

[29] K. He, J. Sun, Computing nearest-neighbor fields via propagation-assisted kd-trees, in: IEEE Conference on Computer Vision and Pattern Recognition (CVPR), IEEE, 2012, pp. 111–118.

[30] Z. Chen, S. Cohen, Y. Wu, H. Jin, Z. Lin, Large displacement optical flow from nearest neighbor fields, in: IEEE Conference on Computer Vision and Pattern Recognition (CVPR), IEEE, 2013, pp. 2443–2450.

[31] L. Bao, Q. Yang, H. Jin, Fast edge-preserving patchmatch for large displacement optical flow, IEEE Transactions on Image Processing (TIP) 23 (2014) 4996–5006.

[32] S. Hong, S. Kwak, B. Han, Orderless tracking through model-averaged posterior estimation, in: International Conference on Computer Vision (ICCV), IEEE, 2013, pp. 2296–2303.

[33] F. Wang, M. Lu, Hamiltonian monte carlo estimator for abrupt motion tracking, in: IEEE International Conference on Pattern Recognition (ICPR), IEEE, 2012, pp. 3066–3069.

[34] N. Sundaram, T. Brox, K. Keutzer, Dense point trajectories by gpu-accelerated large displacement optical flow, in: European Conference on Computer Vision (ECCV), Springer, 2010.

[35] M. Kristan, A. Leonardis, D. Skočaj, Multivariate online kernel density estimation with gaussian kernels, Pattern Recognition 44 (2011) 2630–2642.

[36] F. Liang, C. Liu, R. J. Carroll, Stochastic approximation in monte carlo computation, Journal of the American Statistical Association 102 (2007) 305–320.

[37] F. Liang, Improving samc using smoothing methods: Theory and applications to bayesian model selection problems, The Annals of Statistics 37 (2009) 2626–2654.

[38] J. Kwon, K. M. Lee, Visual tracking decomposition, in: IEEE Conference on Computer Vision and Pattern Recognition (CVPR), IEEE, 2010, pp. 1269–1276.

[39] Y. Wu, J. Lim, M.-H. Yang, Online object tracking: A benchmark, in: IEEE Conference on Computer Vision and Pattern Recognition (CVPR), IEEE, 2013, pp. 2411–2418.

[40] B. Babenko, M.-H. Yang, S. Belongie, Robust object tracking with online multiple instance learning, IEEE Transactions on Pattern Recognition and Machine Intelligence (TPAMI) 33 (2011) 1619–1632.